Check for updates

Femoral Epiphyseal Cartilage Matrix Changes at Predilection Sites of Equine Osteochondrosis: Quantitative MRI, Second-Harmonic Microscopy, and Histological Findings

Gabrielle Martel,[1] Charles-André Couture,[2] Guillaume Gilbert,[3] Stéphane Bancelin,[2] Hélène Richard,[1] Thomas Moser,[4] Sabrina Kiss,[4] François Légaré,[2] Sheila Laverty[1]

[1]Comparative Orthopaedic Research Laboratory, Faculté de médecine vétérinaire, Université de Montréal, Québec, Canada, [2]INRS-EMT, Université du Québec, Québec, Canada, [3]MR Clinical Science, Philips Healthcare, Markham, Ontario, Canada, [4]Department of Radiology, Centre Hospitalier de l'Université de Montréal, Hôpital Notre-Dame, Montréal, Québec, Canada

Received 4 August 2015; accepted 21 January 2016
Published online 8 February 2016 in Wiley Online Library (wileyonlinelibrary.com). DOI 10.1002/jor.23176

ABSTRACT: Osteochondrosis is an ischemic chondronecrosis of epiphyseal growth cartilage that results in focal failure of endochondral ossification and osteochondritis dissecans at specific sites in the epiphyses of humans and animals, including horses. The upstream events leading to the focal ischemia remain unknown. The epiphyseal growth cartilage matrix is composed of proteoglycan and collagen macromolecules and encases its vascular tree in canals. The matrix undergoes major dynamic changes in early life that could weaken it biomechanically and predispose it to focal trauma and vascular failure. Subregions in neonatal foal femoral epiphyses ($n = 10$ osteochondrosis predisposed; $n = 6$ control) were assessed for proteoglycan and collagen structure/content employing 3T quantitative MRI (3T qMRI: T1ρ and T2 maps). Site-matched validations were made with histology, immunohistochemistry, and second-harmonic microscopy. Growth cartilage T1ρ and T2 relaxation times were significantly increased ($p < 0.002$) within the proximal third of the trochlea, a site predisposed to osteochondrosis, when compared with other regions. However, this was observed in both control and osteochondrosis predisposed specimens. Microscopic evaluation of this region revealed an expansive area with low proteoglycan content and a hypertrophic-like appearance on second-harmonic microscopy. We speculate that this matrix structure and composition, though physiological, may weaken the epiphyseal growth cartilage biomechanically in focal regions and could enhance the risk of vascular failure with trauma leading to osteochondrosis. However, additional investigations are now required to confirm this. 3T qMRI will be useful for future non-invasive longitudinal studies to track the osteochondrosis disease trajectory in animals and humans.
© 2016 Orthopaedic Research Society. Published by Wiley Periodicals, Inc. J Orthop Res 34:1743–1752, 2016.

Keywords: epiphyseal growth cartilage; proteoglycan; collagen; quantitative MRI; osteochondrosis

Osteochondrosis is a disorder that affects both human and animal joint development and lesions arise very early in life.[1] As access to osteochondrosis lesion specimens is hampered because of ethical constraints, investigation of the very early stages of the disease in children is limited.[2] However, major advances in knowledge of the pathophysiology of osteochondrosis have been made from animal studies of naturally occuring disease in recent years and the earliest subclinical lesion is now well recognized to be a focal ischemic chondronecrosis of the epiphyseal growth cartilage.[3–6] Normal neonatal epiphyses are composed of an avascular articular cartilage overlying a vascularized growth cartilage.[7,8] With osteochondrosis, the focally ischemic chondronecrotic cartilage fails to undergo endochondral ossification and may form a cartilage flap or osteochondral fragment at the joint surface.[9] At this advanced stage it is termed osteochondritis dissecans.

The upstream events leading to the focal growth cartilage ischemia remain to be elucidated.[10] As cartilage's biomechanical properties are highly dependant on the major structural constituents of its matrix, it is speculated that changes in the epiphyseal growth cartilage matrix macromolecules at specific subregional sites in joints predisposed to osteochondrosis may render the cartilage canals and blood vessels susceptible to trauma and subsequent vascular failure.[7,11] Collagen has been proposed to play a role in the pathogenesis of osteochondrosis (reviewed by Laverty et al.[1]): collagen structural changes may predispose to cartilage canal collapse and ischemia or, altered collagen metabolism may translate to a biomechanically susceptible matrix. Proteoglycan depletion has also been identified at osteochondrosis predilection sites in fœtuses and young foals[7] and, although considered to be a normal developmental feature, may be linked to the onset of the disease.

The horse has a high prevalence of osteochondrosis leading to osteochondral fragments and joint pain in juvenile animals, similar to humans, and is a suitable model for investigations of the naturally occurring disease.[2] Furthermore, osteochondrosis occurs in the distal femoral epiphyses of both humans and horses and usually arises at specific sites and may often be bilateral.[2]

Osteochondrosis lesions have not been identified in the few studies of equine fetuses to date and the youngest foal reported with an osteochondrosis lesion was 2-days-old.[12] Investigations of the causes of osteochondrosis very early after birth may help elucidate if

Grant sponsor: Ministère de l'Agriculture, des Pêcheries et de l'Alimentation du Québec (MAPAQ); Grant sponsor: National Science and Engineering Council of Canada (NSERC); Grant sponsor: Réseau ThéCell; Grant sponsor: Fonds de Recherche en Santé Québec (FRSQ); Grant sponsor: FRQNT.
Correspondence to: Sheila Laverty (T: 450-773-8521 8267; F: 450-778-8158; E-mail: sheila.laverty@umontreal.ca)
© 2016 Orthopaedic Research Society. Published by Wiley Periodicals, Inc.

there is a link between physiological maturation events in the epiphyseal growth cartilage matrix and the onset of osteochondrosis lesions.

Magnetic resonance imaging (MRI) is currently the most suitable imaging modality to evaluate cartilage non-invasively in vivo. MRI studies of epiphyseal development have been performed in children[13] and juvenile animals including pigs,[14–18] lambs,[19] rabbits,[20] and horses.[8,21] A variety of sequences have been identified to better distinguish the articular, epiphyseal, and physeal cartilage.[13]

Quantitative MRI (qMRI) reveals site variations of proteoglycan content (T1ρ maps) and collagen structure (T2 maps). Quantitative T1ρ has been employed for the early diagnosis of cartilage degeneration and was shown to be sensitive to changes in cartilage proteoglycan content (reviewed by Li and Majumdar[22]). Recently, 9.4T T1ρ, adiabatic T1ρ and T2 relaxation time mapping permitted the identification of cartilage necrosis following surgical interruption of the vascular supply of the distal femoral epiphyseal growth cartilage of juvenile goats for the first time.[23] T2 mapping has been employed for the assessment of cartilage development in humans and other species and has revealed that juvenile articular cartilage has a multi-laminar appearance of up to seven layers due to incomplete maturation and structural variations.[24,25] However, qMRI with both T1ρ and T2 mapping sequences has never been employed to study naturally occuring osteochondrosis in any species or in equine epiphyseal cartilage to date.

We hypothesize that osteochondrosis predilection regions in the epiphyseal cartilage of neonatal foals have physiological variations in proteoglycan and collagen structure or content that could be implicated in the early pathogenesis of the disease.

The specific objectives of this study were twofold: To investigate the proteoglycan content and collagen content and structure of the epiphyseal cartilage of the femoral trochlea in control foals and neonatal foals predisposed to osteochondrosis employing q3T MRI (T1ρ and T2 maps) and to validate the imaging findings with site-matched second-harmonic microscopy for collagen ultrastructure, immunohistochemistry for type II collagen, and histology for proteoglycan content.

MATERIALS AND METHODS

Animal and Collection Procedures

The experimental protocol was approved by the institutional animal care and use committee. Furthermore, guidelines established by the Canadian Council on Animal Care were strictly followed. Foals ($n = 5$; osteochondrosis predisposed group) were conceived by embryo transfer from three Standardbred donor mares and a Standardbred stallion, all with a history of osteochondritis dissecans lesions (Table SI). The foals were humanely euthanized with an IV injection of embutramide (75 mg/kg) within 24 h of birth, following deep sedation of both the dams and the foals with xylazine (0.6 mg/kg IV). Control animals were foals ($n = 4$) that died at the veterinary teaching hospital from other causes. The osteochondrosis status of parents in this group was negative according to foals' owners. The mean age of the control foals was 2 days. Breed and the cause of death are provided in Table SI (supplementary information online). Hindlimbs were disarticulated at the coxofemoral joint and kept in a refrigerator and then frozen at −20°C until imaging and thawed prior to MRI.

MRI

Sixteen hindlimbs ($n = 6$ control and 10 osteochondrosis predisposed) were oriented parallel to the main magnetic field and the stifles were imaged with a 3T MRI (Achieva X, Philips Healthcare, Best, The Netherlands) with a maximum gradient strength of 40 mT/m, a maximum slew rate of 200 T/m/s and an eight-channel receive only knee coil.

T1ρ mapping was performed using a 2D multi-slice magnetization-prepared steady-state free precession sequence with seven different spin-locking times (1, 10, 20, 30, 40, 50, 60 ms). Spin-locking was performed at a frequency of 500 Hz by using a rotary echo locking scheme. Local shimming was performed specifically on the region of interest (ROI) to improve B0 homogeneity. Other imaging parameters were: TR = 5.0 ms, TE = 2.5 ms, flip angle = 40 degrees, field-of-view = $140 \times 140\,mm^2$, resolution = $0.55 \times 0.55\,mm^2$, slice thickness = 3 mm, number of slices = 27, acquisition time = 1 min 57 s per spin-locking time.

T2 mapping was performed using a 2D multi-slice multi-echo spin-echo sequence with six different echo times (13, 26, 39, 52, 65, 78 ms). Other imaging parameters were: TR = 2000 ms, flip angle = 90 degrees, field-of-view = $140 \times 140\,mm^2$, resolution = $0.55 \times 0.55\,mm^2$, slice thickness = 3 mm, number of slices = 27, acquisition time = 19 min 52 s.

Cylindrical regions of interest (ROIs) were manually drawn on both the T1ρ and T2 relaxation time maps with ITK-SNAP (http://www.itksnap.org) at proximal, middle, and distal sites in the growth cartilage, just below the articular surface, in both the lateral ($L_{proximal}$, L_{middle}, and L_{distal}) and medial ($M_{proximal}$, M_{middle}, and M_{distal}) ridge of the trochlea. An additional ROI was also assessed deeper to the proximal and middle trochlea sites, close to the junction of the physis and epiphyseal growth cartilage, as the cartilage was very thick in this site (L_{deep}, M_{deep}) (Fig. 1A and B). Clinical osteochondritis dissecans lesions usually occur at the $L_{proximal}$ and L_{middle} ROIs[26] that overly the L_{deep} region.

The ROIs were 243 voxels or $139.535\,mm^3$. T1ρ and T2 relaxation time maps were calculated by means of mono-exponential two-parameter fitting (MatLab 6.5.1, MathWorks Inc., Natick, MA).

Histology: Safranin O Fast Green

Following MR imaging, femurs were dissected free of soft tissues. The femoral trochlea was sectioned in the transverse plane to obtain 0.5–1 cm thick slabs that matched the ROIs. The slabs were fixed in 10% formalin (24 h), decalcified in EDTA (6–7 days), fixed in 70% alcohol (24 h) and embedded in paraffin as described previously.[7] Four micrometer thick sections were cut from each slab and stained with safranin O fast green. A validation of safranin O staining of proteoglycan was also performed with toluidine blue on selected sections with matrix pallor (see later) (Fig. S1). Staining with hematoxylin and eosin at each ROI was also performed to evaluate the presence of chondronecrosis within the growth cartilage. All the sections were digitalized using a Leica DM4000B microscope attached to a Leica DFC320 video camera.

1554527x, 2016, 10, Downloaded from https://onlinelibrary.wiley.com/doi/10.1002/jor.23176 by Portail BibCNRS INP, Wiley Online Library on [11/04/2025]. See the Terms and Conditions (https://onlinelibrary.wiley.com/terms-and-conditions) on Wiley Online Library for rules of use; OA articles are governed by the applicable Creative Commons License

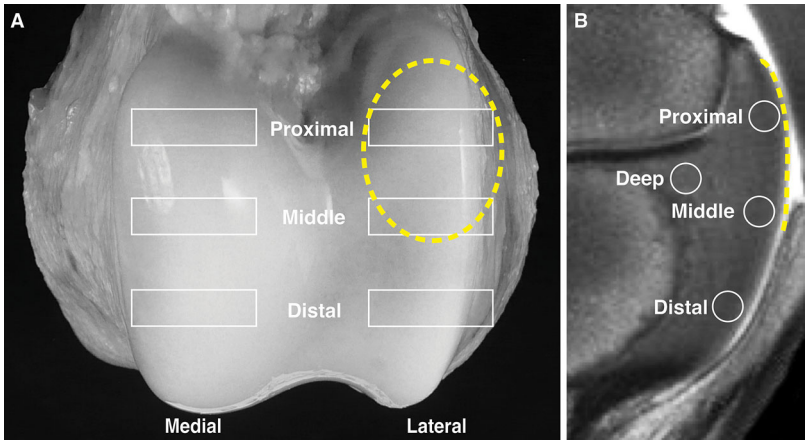


Figure 1. Study design illustrating subregions investigated. (A) Distal femoral trochlea illustrating rectangular regions of interest (ROIs: Proximal, middle, and distal) selected for MRI and histologic investigations in the lateral and medial ridges. Yellow broken oval illustrates the region where osteochondritis dissecans lesions most frequently occur. (B) Sagittal MRI map of a trochlea ridge with ROIs that were assessed by 3T quantitative MRI. It includes the proximal, middle and distal ROIs described in (A). An additional ROI (deep) was assessed because of the thickness of the epiphyseal growth cartilage in this area. The yellow broken line illustrates the region where osteochondritis dissecans lesions most frequently occur.

Immunohistochemistry: Collagen Type II

Selected sections from ROIs that had the greatest T2 mapping variations ($L_{proximal}$, $M_{proximal}$, L_{middle}, and M_{middle}) were immunostained with collagen type II rabbit primary antibody (Abcam inc, Cambridge, MA) (see supplementary information online for protocol).

Second-Harmonic Microscopy

Second-harmonic microscopy (see Brown et al. [2014][27]) was employed to image 10 μm thick tissue slices corresponding to the ROIs. The signal intensity provides information (resolution of 500 nm) on collagen density and alignment over regions of 300×300 μm. The polar plots of this intensity as a function of incident laser polarization provide the general axis of alignment of the fibrils and their anisotropy in the field of view considered. These properties were calculated over each region of 100×50 μm in the images and represented as an arrow whose direction corresponded to the main fibrillar direction, and length indicated the degree of anisotropy of the fibrils within a region. A longer arrow indicates greater anisotropy of the signal, representing a high level of collagen alignment.

Statistical Analysis

A linear mixed model was used to detect differences in T1ρ relaxation time or T2 relaxation time between ROIs in both control and osteochondrosis predisposed groups and to evaluate if there was a difference in T1ρ or T2 relaxation time between the groups at each ROI. To take into account the dependent nature of the samples, the individual was used as a random effect and the ROI as intra-subject factor and the group as factor between specimens. A priori contrasts were used to examine differences between pairs of means adjusting the alpha value for each contrast with the sequential Bonferroni adjustment procedure. A value of $p < 0.05$ was considered significant. All analyses were performed with commercial statistical software (SAS, version 9.3, SAS Institute Inc, Cary, NC).

RESULTS

T1ρ Mapping

T1ρ maps varied between and within articular, epiphyseal, and physeal cartilage revealing very evident differences in proteoglycan content in these zones (Fig. 2). An inverse relationship exists between T1ρ relaxation times and proteoglycan content.[22] The growth cartilage of the proximal and middle ROIs, in both the lateral and medial ridges, had distinct areas with high T1ρ relaxation times (Fig. 2A and B). Transverse projections of the proximal trochlea ROIs confirmed and extended these findings. A central expansive area with increased T1ρ relaxation times was most evident at the ROI $L_{proximal}$ (Fig. 2C) and the area of the zone decreased further distally in the ROI L_{middle} (Fig. 2E). In addition, the T1ρ relaxation times were also elevated in a thin layer close to the metaphyseal ossification front (Fig. 2C). The distal trochlea had overall lower T1ρ relaxation times, except for focal sites in the M_{distal} region (Fig. 2G).

There were no significant differences between the ROI T1ρ relaxation times of the osteochondrosis predisposed and control group. The ROI data of all the specimens were subsequently pooled for further comparisons between sites and within joints (Table SII). There were significant differences in T1ρ relaxation times between the ROIs (Table SIII and Fig. 3B). The highest T1ρ relaxation times were recorded in the ROIs L_{deep} and M_{deep}. The greatest variation in T1ρ relaxation times was observed within the lateral ridge of the trochlea: $L_{proximal}$ values were significantly higher than those of L_{distal}, where the lowest mean values were measured. This pattern was not observed in the medial ridge of the trochlea. The ROI M_{distal} had significantly higher T1ρ relaxation times when compared with L_{distal}.

Histologic Validation of Proteoglycan Content

Safranin O fast green stained slides revealed focal areas with low stain uptake in the growth cartilage indicative of a low proteoglycan content that corresponded to the high relaxation times observed on T1ρ matched maps (Fig. 2C–H).

$L_{proximal}$ sections had a laminar loss of staining in the early proliferative cartilage next to the metaphyseal physis but the matrix staining in areas with hypertrophic chondrocytes was not decreased (Figs. 2D and S2). A central matrix pallor was also seen within the $L_{proximal}$ and the L_{middle} regions in all of the specimens and occasionally also in the M_{middle}

1554527x, 2016, 10, Downloaded from https://onlinelibrary.wiley.com/doi/10.1002/jor.23176 by Portail BibCNRS INP, Wiley Online Library on [11/04/2025]. See the Terms and Conditions (https://onlinelibrary.wiley.com/terms-and-conditions) on Wiley Online Library for rules of use; OA articles are governed by the applicable Creative Commons License

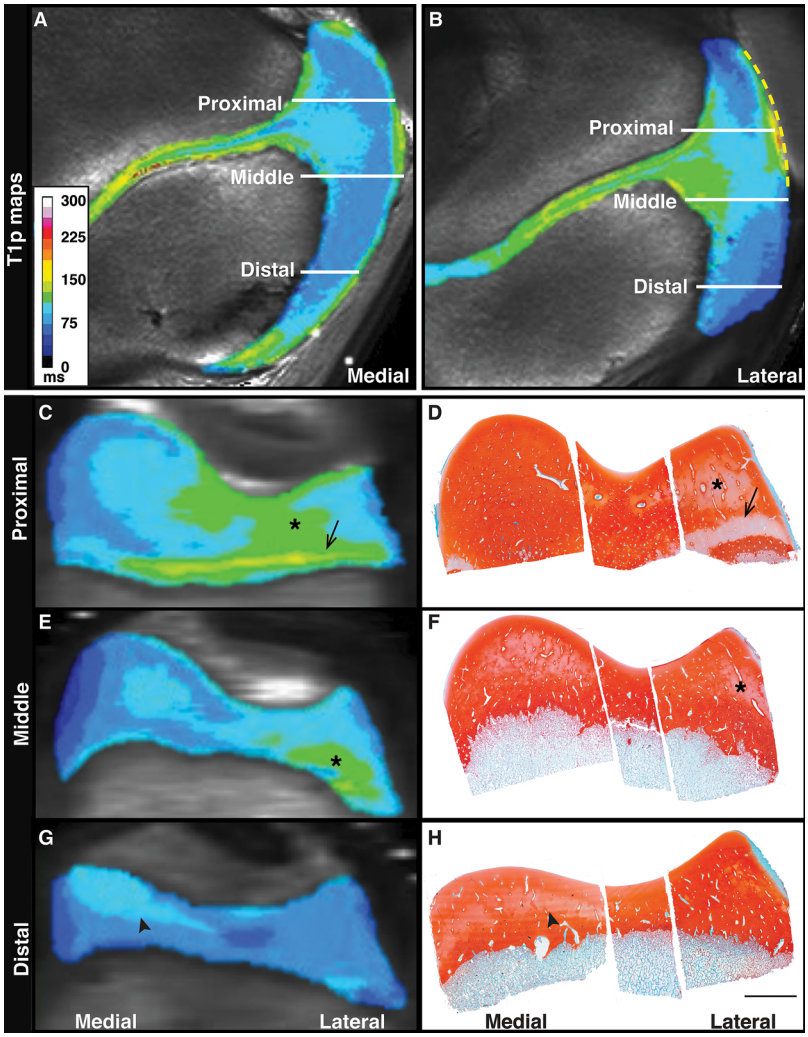


Figure 2. T1ρ maps of proteoglycan content of the epiphyseal growth cartilage in both ridges of the trochlea. (A and B) T1ρ sagittal map of the medial and lateral ridges of the femoral trochlea. Color scale corresponds to T1ρ relaxation times. Longer T1ρ relaxation times reflect lower proteoglycan content. The growth cartilage of the proximal and middle ROIs, in both trochlear ridges, has distinct areas with high T1ρ relaxation times. The highest T1ρ relaxation times are located at the osteochondritis dissecans predilection region (yellow dotted line) in the lateral ridge of the trochlea. (C and D) Transverse T1ρ maps of the proximal ROIs with corresponding site-matched safranin O fast green stained sections. At the ROI $L_{proximal}$, lower proteoglycan content (increased T1ρ relaxation times and low safranin O staining uptake) is visible within a central area (asterisk) and also in a thin layer close to the metaphyseal ossification front (arrow). (E and F) Transverse T1ρ maps of the middle ROIs with corresponding site-matched safranin O fast green stained sections. Increased T1ρ relaxation times are still observed within the ROI L_{middle} (asterisk). (G and H) Transverse T1ρ maps of the distal ROIs with corresponding site-matched safranin o fast green stained sections. There is overall lower T1ρ relaxation times and homogeneous stain uptake in the matrix, except for small focal sites in the M_{distal} (arrow head). Scale bar = 1 cm.

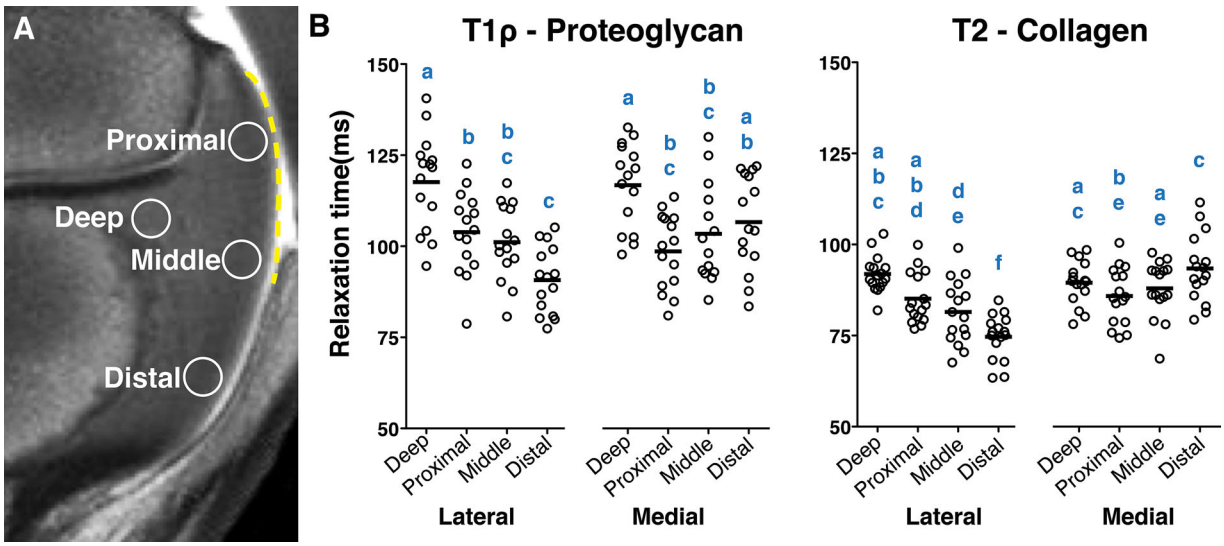


Figure 3. T1ρ and T2 relaxation times (ms) at ROIs in the femoral trochlea. (A) Sagittal map indicating ROIs used for quantitative MRI assessment. The yellow broken line illustrates the region where osteochondritis dissecans lesions most frequently occur. (B) Dot plots of T1ρ and T2 relaxation times (ms) at each ROI. An inverse relationship exists between T1ρ relaxation times and proteoglycan content. An increase of the T2 relaxation times is associated with a decrease of collagen content and anisotropy. A linear mixed model was used, with the individual as a random effect, the ROI as an intra-subject factor and the group as a factor between specimens to detect differences in T1ρ relaxation times or T2 relaxation times between ROIs in both control and osteochondrosis predisposed groups. Means that share superscript letters are not significantly different ($p > 0.05$).

1554527x, 2016, 10, Downloaded from https://onlinelibrary.wiley.com/doi/10.1002/jor.23176 by Portail BibCNRS INP, Wiley Online Library on [11/04/2025]. See the Terms and Conditions (https://onlinelibrary.wiley.com/terms-and-conditions) on Wiley Online Library for rules of use; OA articles are governed by the applicable Creative Commons License

(Fig. 2D and F). Sections from the distal sites of both ridges of the trochlea had good stain uptake in the majority of the specimens, but a few M_{distal} sections had focal areas of matrix pallor (Fig. 2H). The loss of proteoglycan within the areas of low safranin O staining uptake was also confirmed on selected site-matched sections stained with toluidine blue (Fig. S1). Chondronecrosis assessed on hematoxylin and eosin sections was not found within any of the areas of matrix pallor (Fig. S2).

T2 Mapping

T2 mapping revealed a variation of T2 relaxation times between and within articular, epiphyseal, and physeal cartilage (Fig. 4). An increase of the T2 relaxation times is associated with a decrease of collagen anisotropy and/or content.[28] The articular cartilage had higher T2 values than those of the underlying growth cartilage, permitting easy differentiation of the two, and had a bilaminar appearance (Fig. 4A, site 1). The growth cartilage had homogeneous lower T2 values (Fig. 4B, site 2). The ROI M_{deep} had small focal areas with higher T2 relaxation times and ROI L_{deep} presented overall high T2 relaxation times (Fig. 4A, site 3 and B, site 4).

There were no significant differences between the ROI T2 relaxation times of the osteochondrosis predisposed and control group. The information from all the ROIs was then pooled for further statistical analyses (Table SII). There were significant differences in T2 relaxation times between the ROIs (Table SIV and Fig. 3B). ROIs L_{deep} and M_{deep} had the highest T2 relaxation times. The greatest variation in T2 relaxation times was also observed within the ROIs in the lateral ridge of the trochlea: $L_{proximal}$ values were significantly higher than those of the L_{distal} where the lowest mean values were measured, but this pattern was not observed in the medial ridge of the trochlea.

Second-Harmonic Microscopic Validation of Collagen Structure

The second-harmonic signal variations corroborated those observed on T2 maps. The bilaminar pattern of the articular cartilage on T2 maps corresponded to the increased signal from the superficial, transitional, and radial layers (Fig. 4A, site 1 and C, zones i–iii) and to

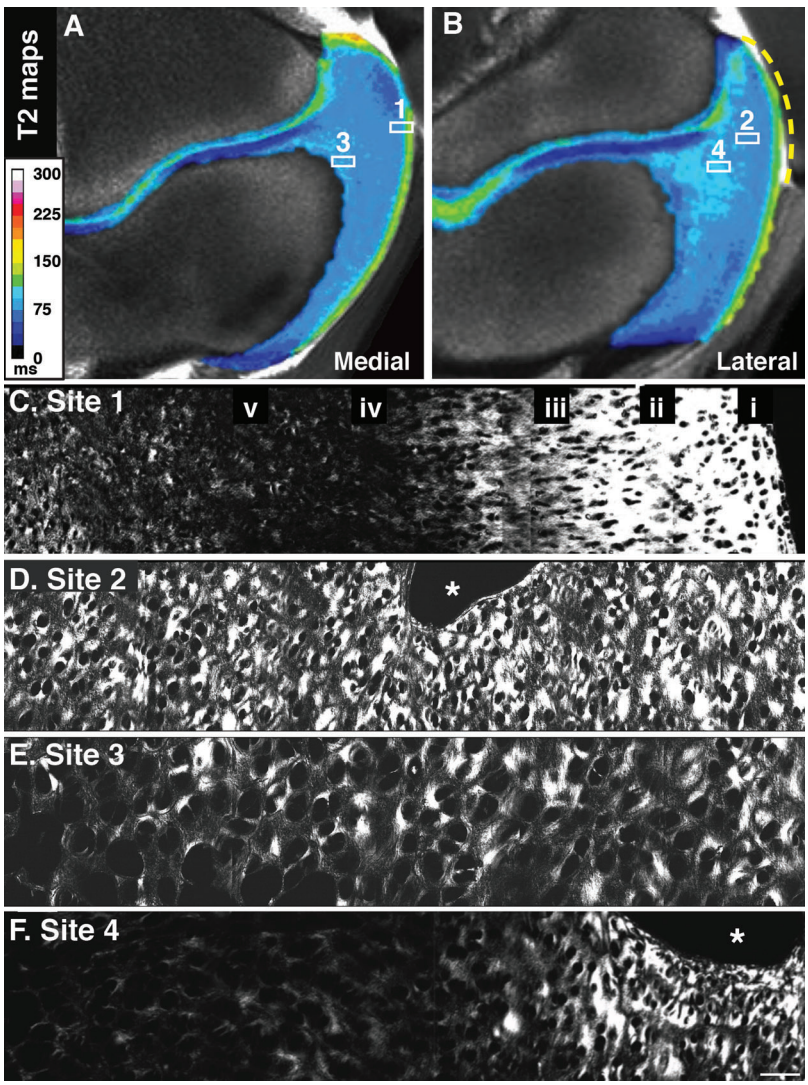


Figure 4. Mapping of collagen structure of epiphyseal growth cartilage of the femoral trochlea. (A and B) Representative T2 sagittal maps of the lateral and medial ridges of the femoral trochlea. Rectangles 1–4 in the images represent the sites examined by second-harmonic microscopy. An increase of the T2 relaxation times is associated with a decrease of collagen content and anisotropy. (C) Site 1. Laminar appearance of articular cartilage visible on T2 map and second-harmonic microscopy scan. The collagen is denser at the articular surface and a change in chondrocyte lacunae shape is evident from the surface to the deeper layers (i. superficial; ii. transitional; iii. radial; iv. deeper transitional layers; and v. epiphyseal cartilage). Note also the small size of the chondrocyte lacunae. (D) Site 2. Homogeneous T2 values and second-harmonic signal of the epiphyseal cartilage. White asterik represents a blood vessel in a cartilage canal. (E) Site 3. Epiphyseal cartilage at the ROI M_{deep} with focal increase of T2 values and decrease of second-harmonic signal. The chondrocyte lacunae are very large, when compared to those nearer the articular surface (C) and represent hypertrophic cartilage. (F) Site 4. Epiphyseal cartilage at the ROI L_{deep} with expansive increase of T2 values and decrease of second-harmonic signal indicating lower collagen content or anisotropy. A dramatic increase in chondrocyte lacunae size and change in shape occurs from right to left corresponding to chondrocyte hypertrophy. White asterik represents a blood vessel in a cartilage canal. Scale bar = 0.1 mm.

1554527x, 2016, 10, Downloaded from https://onlinelibrary.wiley.com/doi/10.1002/jor.23176 by Portail BibCNRS INP, Wiley Online Library on [11/04/2025]. See the Terms and Conditions (https://onlinelibrary.wiley.com/terms-and-conditions) on Wiley Online Library for rules of use; OA articles are governed by the applicable Creative Commons License

the loss of signal within the deeper transitional layer (Fig. 4A, site 1 and C, zone iv). The growth cartilage had a homogenous second-harmonic signal (Fig. 4B, site 2 and D). Epiphyseal cartilage at the ROI M_{deep} had small focal areas with an increase of T2 values corresponding to the decreased second-harmonic signal and hypertrophic chondrocyte lacunae (Fig. 4A, site 3 and E). The higher T2 values at the ROI L_{deep} corresponded to a zone with low second-harmonic signal and large chondrocyte lacunae shape with an organization similar to that of the hypertrophic zone (Fig. 4B, site 4 and F). This hypertrophic-like region extended more cranially at the ROI L_{deep}, compared to elsewhere along the secondary ossification front (Fig. 5A, sites 2–4 and C–E). The metaphyseal ossification front cartilage at the ROI $L_{proximal}$ presented distinct very large and aligned hypertrophic chondrocyte lacunae (Fig. 5A, site 1 and B) compared to those of the secondary ossification centre that are randomly distributed (Fig 5A, site 5 and F).

Immunohistochemistry for Type II Collagen

Selected site-matched type II collagen immunostained sections from the ROIs $L_{proximal}$ and L_{middle} revealed type II collagen staining centrally where the T2 relaxation times were low (Fig. 6A, B, D, and E). Second-harmonic microscopy scans within these areas revealed an enhanced signal and increased collagen anisotropy (Fig. 6C) compared to the extended hypertrophic cartilage near the ossification front (Fig. 6F).

DISCUSSION

The findings of this study provide a number of novel insights into equine epiphyseal development pertinent to the understanding of osteochondrosis in all species. qMRI revealed that the epiphyseal growth cartilage matrix composition and structure varies substantially between the proximal, middle, and distal aspects of the trochlea of the femur. The lateral ridge had the greatest variation. Classical lesions of osteochondritis dissecans occur most frequently in the lateral ridge of the equine femoral trochlea compared to the medial ridge.[26,29–31] This investigation is, to the best of our knowledge, the first to examine, in parallel, growth cartilage proteoglycan content, collagen content, and collagen structure employing qMRI with validation by histology, immunohistochemistry, and second-harmonic microscopy in any species. Second-harmonic microscopy provided evidence of a strong link between the T2 mapping variations and collagen structural variation within and between articular, epiphyseal, and physeal cartilage.

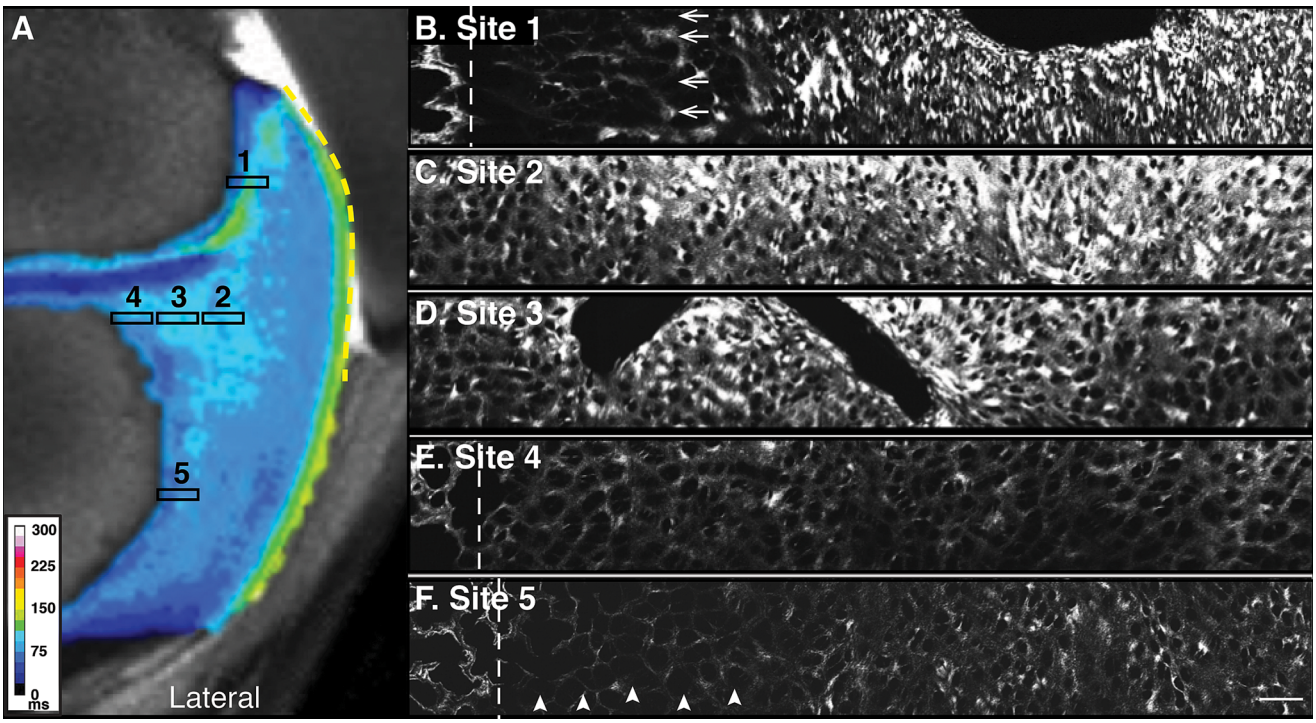


Figure 5. The osteochondral junction zone of the proximal, middle, and distal femoral trochlea of the lateral ridge of the trochlea of the femur. (A) Sagittal T2 map of the lateral ridge of the trochlea. Rectangles 1–5 in the image represent the sites examined by second-harmonic microscopy. (B) Site 1. Second-harmonic scan of the metaphyseal ossification front at the ROI $L_{proximal}$. From right to left of the second-harmonic scan, the collagen structure becomes less dense and the chondrocyte lacunae change dramatically in shape and size. The hypertrophic chondrocyte lacunae are very large and aligned at the left (arrows). White dotted line is the osteochondral junction. (C–E) Site 2–4. Consecutive second-harmonic scans of the cranio-proximal aspect of the second ossification centre at the ROI L_{deep}. White dotted line is the osteochondral junction. When compared to site 1, it is evident that the hypertrophy (enlarged chondrocyte lacunae) extends over a much larger area in this region. (F) Site 5. Second-harmonic scan of the secondary ossification centre at the ROI L_{distal}. The hypertrophic region is much narrower in this region and the hypertrophic chondrocytes are randomly distributed (arrow heads). White dotted line is the osteochondral junction. Scale bar = 0.1 mm.

1554527x, 2016, 10, Downloaded from https://onlinelibrary.wiley.com/doi/10.1002/jor.23176 by Portail BibCNRS INP, Wiley Online Library on [11/04/2025]. See the Terms and Conditions (https://onlinelibrary.wiley.com/terms-and-conditions) on Wiley Online Library for rules of use; OA articles are governed by the applicable Creative Commons License

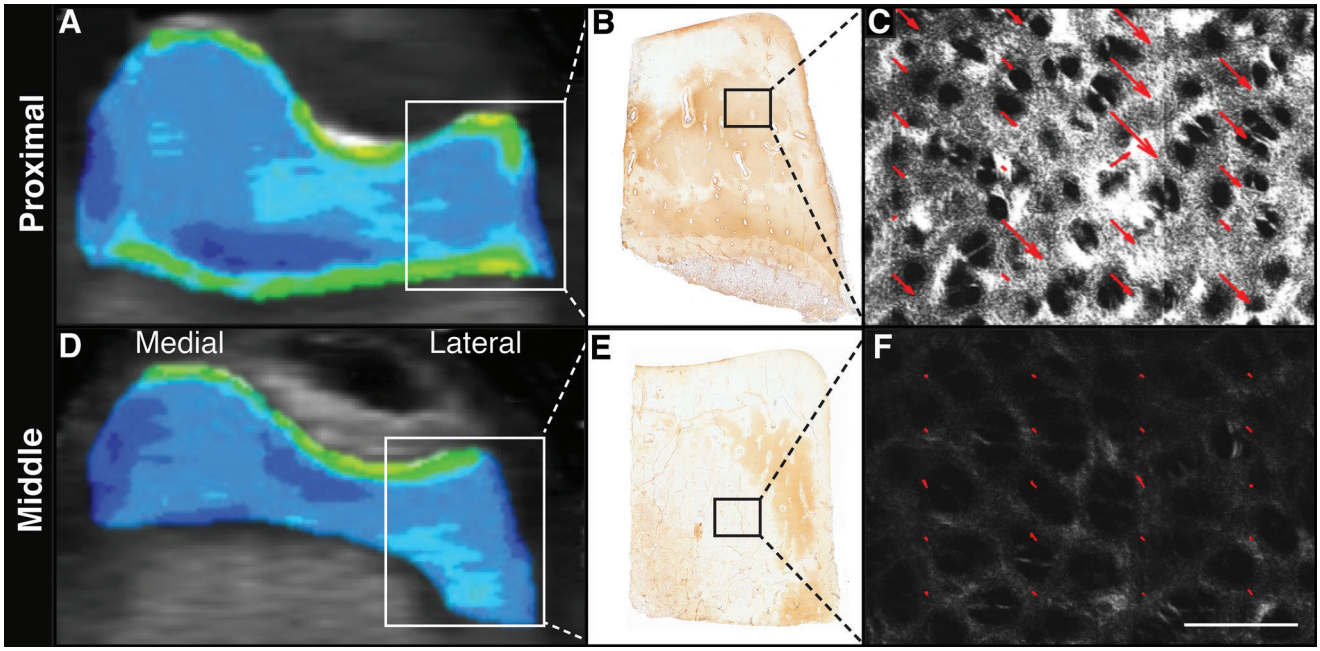


Figure 6. Epiphyseal growth cartilage matrix remodeling in the proximal and middle regions of the lateral ridge of the trochlea. (A and B) T2 transverse map and type II collagen immunohistochemistry of the ROI $L_{proximal}$ demonstrating a central area with enhanced collagen immunostaining and low T2 relaxation times. (C) Second-harmonic microscopy of rectangle in (B). Red arrows represent predominant collagen orientation and their length is proportional to collagen anisotropy. There is enhanced second-harmonic signal and collagen anisotropy. (D and E) T2 transverse map and type II collagen immunohistochemistry of the ROI L_{middle} demonstrating reduced collagen immunostaining and high T2 relaxation times along the cranio-proximal aspect of the secondary center of ossification where osteochondritis dissecans frequently arises. (F) Second-harmonic microscopy of rectangle in (E). Red arrows represent predominant collagen orientation and their length is proportional to collagen anisotropy. There is a loss of collagen anisotropy and larger chondrocyte lacunae representing hypertrophic-like cartilage. Scale bar = 0.1 mm.

Despite efforts to create an osteochondrosis phenotype, no classical early histological lesions of osteochondrosis were detected in either group. This may have been due to the small number of animals studied because of ethical constraints or to the very early timepoint of the investigation. As this was a terminal and exploratory study, we tried to reduce the number of animals sacrificed for ethical reasons. However, it is recognized that a larger number of animals may have yielded different results. On the other hand, the fact that several joints from each animal could be analyzed increased the power of our study.

Our study design to increase the number of osteochondrosis predisposed foals was an extension of those reported previously[32,33] where sires and dams with OCD were bred. The reported prevalence of microscopic osteochondrosis in the femoropatellar joint of young foals with affected parents is 28% and 0% in foals from non-affected parents.[30] As osteochondrosis lesions have been observed in a 2-day-old foal,[12] we believed at the outset that we might identify early lesions in these foals. Although we did not detect early lesions with our methods, it remains possible that the specimens may contain early, but as yet un-characterized, molecular, or cellular upstream events that lead to classical early osteochondrosis histological lesions. Despite these limitations, our findings illustrate the development of the osteochondrosis predilection sites and provide a foundation for future studies to investigate the link between the growth cartilage matrix changes, its biomechanical properties and the early vascular ischemic events of osteochondrosis.

A large zone of low proteoglycan content, but with homogeneous type II collagen immunostaining and increased anisotropy, was identified in the epiphyseal cartilage at the proximal trochlea sites, where clinical osteochondritis dissecans lesions arise,[26] and was observed with multiple modalities. However, it was observed in both osteochondrosis predisposed and control specimens, suggesting that these matrix variations may be part of physiologic maturation of the trochlea.[7] These findings confirm and extend those of a previous histological study of equine epiphyseal maturation in fœtuses and foals.[7] Focal areas of low proteoglycan content were observed within osteochondrosis predilection sites in different joints, but were more prevalent in the femoropatellar joint.[7,8] The growth cartilage matrix changes were associated with age: their prevalence decreased with the time of gestation, but they remained present at birth in the distal femur reflecting the late maturation of this joint.[7] However, unlike the expansive regions of growth cartilage pallor we observed in the study herein, the focal areas observed by Lecocq et al. (2008)[7] were localized close to chondrifying canals, similar to other investigations of the normal appear-

1554527x, 2016, 10, Downloaded from https://onlinelibrary.wiley.com/doi/10.1002/jor.23176 by Portail BibCNRS INP, Wiley Online Library on [11/04/2025]. See the Terms and Conditions (https://onlinelibrary.wiley.com/terms-and-conditions) on Wiley Online Library for rules of use; OA articles are governed by the applicable Creative Commons License

ance of epiphyseal cartilage in osteochondrosis affected species.[34,35]

It remains to be elucidated whether the large zones with low proteoglycan are a result of increased proteoglycan turnover or reduced synthesis. Growth plate matrix remodeling and the interrelationships between its extracellular matrix synthesis, proteinases, and their inhibitors, has been studied in many species.[36–39] However, no age-related studies of proteoglycan distribution in equine growth carilage have been reported. Gene expression studies at different zones of the growth plate of bovine fetuses[36] recently revealed that aggrecan synthesis occurred in the resting zone and was initially decreased, and later absent, in the proliferative zone. The synthesis was upregulated again at the onset of chondrocyte hypertrophy. In situ hybridization studies of aggrecan expression in the human growth plate during different stages of human skeletal development also showed that the resting zone had the lowest expression and a higher expression occurred in the lower proliferative and upper hypertrophic zone.[40] The focal zones of growth cartilage pallor (less proteoglycan) we observed herein contained resting and proliferative chondrocytes. Although they are potentially related to normal physiological developmental changes in epiphyseal growth cartilage, their patchy distribution suggests otherwise.

An alternative explanation for the focal zones of matrix pallor observed with both qMRI and Safranin O staining is a focal extracellular matrix resorption, similar to that observed in rodent epiphyseal growth cartilage.[41] Two forms of resorption were observed: "free", not associated with ossification events, and "ossification–coupled resorption" occurring at the secondary ossification center front and the primary growth plate. The latter proteolytic resorption is due to aggrecanase and MMP activity.[41] The subregional proteoglycan depletion observed in the study herein resembles "free" resorption and may allow expansion of the secondary ossification center, but this remains to be confirmed.

We also identified an expansive hypertrophic-like zone on T2 maps and second harmonic microscopy extending abaxially in the lateral ridge of the trochlea at the cranio-proximal aspect of the secondary ossification centre that has not been described before. It is known that the hypertrophic zone of the physeal cartilage is the least rigid region of the growth plate[42] and that the physeal osteochondral junction is less resistant to shear forces and more likely to fracture than adult tissue.[43,44] This biomechanical weakness is due to a physiological zonal loss of cartilage matrix because of a concurrent dramatic increase in chondrocyte volume (chondrocyte hypertrophy) with accompanying proteolysis and resorption of collagen in the process of endochondral ossification.[1] It is of interest that, in a parallel study employing susceptibility-weighted imaging of the same specimens[45] to map 3D vascularity of the growth cartilage, this hypertrophic-like zone contains many perichondral vessels that are known to be vulnerable to vascular failure as they get incorporated into the ossification front with ongoing ossification.[5]

This study underpins the clinical potential of T1ρ and T2 mapping for identifying and monitoring abnormal cartilage growth and ossification in children. Subregional matrix variations similar to the changes we describe here have also been identified on T2 maps of the femoral condyle of children, a site of predilection for osteochondritis dissecans, but no further histological validation of the MRI findings could be performed for ethical reasons.[2] The study herein confirms and extends these findings by adding ex vivo comparisons of imaging with histology, immunohistochemistry, and second-harmonic microscopy in an animal model.

Taken together, the results of our investigations suggest that the growth cartilage at the cranio-proximal aspect of the secondary ossification centre in the lateral ridge of the equine femoral trochlea has a distinct matrix composition at birth. These subregional matrix variations may be associated with growth spurts and decrease the epiphyseal cartilage mechanical properties subregionally as recently illustrated in the ulnar physis of growing pigs.[46] We speculate that a temporary focal weakening of the epiphyseal cartilage could predispose the vessels, housed within, to injury precipitating the early ischemic events of osteochondrosis. As both the control and osteochondrosis predisposed foals had these cartilage matrix characteristics at birth, vascular failure and osteochondrosis onset could be triggered by an additional cofactor such as biomechanical stresses from internal (joint geometry) or external trauma later in the foal's life.[10] An example of internal trauma due to abnormal anatomy leading to joint pathology is provided by femoracetabular impingement in adolescents which is now believed to be due to variations in hip anatomy resulting in mechanical aberrations of joint function.[47] Similar events could be at play in joints with osteochondrosis. Additional investigations are now needed to understand the changes in the cartilage matrix composition during maturation and, importantly, the associated variations in its biomechanical properties over time.

In conclusion, we have identified focal epiphyseal growth cartilage matrix changes, including regions with low proteoglycan and also, previously undescribed, large hypertrophic cartilage zones with less collagen, in the equine femoral trochlea at osteochondritis dissecans predilection sites. These focal changes could potentially weaken the growth cartilage and predispose the vessels, housed within, to injury precipitating the early ischemic events of osteochondrosis. Additional biomechanical studies are now planned to investigate this further. qMRI and complementary MRI SWI for mapping of the vascular tree of growth cartilage[45] are both clinically feasible and non-invasive and may be employed for future longitudinal studies

1554527x, 2016, 10, Downloaded from https://onlinelibrary.wiley.com/doi/10.1002/jor.23176 by Portail BibCNRS INP, Wiley Online Library on [11/04/2025]. See the Terms and Conditions (https://onlinelibrary.wiley.com/terms-and-conditions) on Wiley Online Library for rules of use; OA articles are governed by the applicable Creative Commons License

to investigate the link between the matrix changes of growing cartilage we have identified and the later development of osteochondrosis and expand the understanding of underlying etiology of osteochondrosis in humans.

AUTHORS' CONTRIBUTIONS

GM collected the specimens, performed the descriptive and quantitative MRI analyses and microscopic validation and wrote the manuscript. CAC performed the second harmonic generation microscopy analyses. GG conceived the imaging acquisition and processing protocol and revised the manuscript. SB assisted in the the second harmonic generation microscopy analyses. HR prepared the histologic and immunohistochemic specimens. TM participated in the study design and evaluated the MRI images. SK evaluated the MRI images. FL participated in the study design. SL conceived and designed the study, evaluated the histological specimens, and revised the manuscript. All authors have read and approved the final submitted manuscript.

ACKNOWLEDGMENTS

We would like to thank the following people for their contributions: Danielle Blain for her technical assistance with MRI, Dr. Claude Forget DVM for procuring osteochodrosis affected animals, Dr. Rejean Lefebvre DVM PhD DACVR for embryo transfer, Dr. Christiane Girard DVM DACVP for valuable insight on the histological assessment of the tissues and Dr. Guy Beauchamps for statistical analyses.

This project was funded in part by Ministère de l'Agriculture, des Pêcheries et de l'Alimentation du Québec (MAPAQ), Quebec. Sheila Laverty's laboratory is currently funded by the National Science and Engineering Council of Canada (NSERC), the Réseau ThéCell, Fonds de Recherche en Santé Québec (FRSQ) and also by a generous gift from Mr. and Mrs. J. Magnier, Coolmore Stud, Fethard, Ireland. The authors acknowledge supports from Canada Foundation for Innovation for the nonlinear optical microscope available at INRS-ÉMT, financial supports from NSERC and FRQNT. Furthermore, CAC acknowledges supports from NSERC and FRQNT for M.Sc. student awards.

REFERENCES

1. Laverty S, Girard C. 2013. Pathogenesis of epiphyseal osteochondrosis. Vet J 197:3–12.
2. McCoy AM, Toth F, Dolvik NI, et al. 2013. Articular osteochondrosis: a comparison of naturally occurring human and animal disease. Osteoarthritis Cartilage 21:1638–1647.
3. Olstad K, Ytrehus B, Ekman S, et al. 2011. Early lesions of articular osteochondrosis in the distal femur of foals. Vet Pathol 48:1165–1175.
4. Carlson CS, Hilley HD, Meuten DJ. 1989. Degeneration of cartilage canal vessels associated with lesions of osteochondrosis in swine. Vet Pathol 26:47–54.
5. Ytrehus B, Ekman S, Carlson CS, et al. 2004. Focal changes in blood supply during normal epiphyseal growth are central in the pathogenesis of osteochondrosis in pigs. Bone 35: 1294–1306.
6. Weiss S, Loeffler K. 1996. [Histological study of cartilage channels in the epiphyseal cartilage of young dogs and their relationship to that of osteochondrosis dissecans in the most frequently affected locations]. Dtsch Tierarztl Wochenschr 103:164–169.
7. Lecocq M, Girard CA, Fogarty U, et al. 2008. Cartilage matrix changes in the developing epiphysis: early events on the pathway to equine osteochondrosis? Equine Vet J 40:442–454.
8. Cluzel C, Blond L, Fontaine P, et al. 2013. Foetal and postnatal equine articular cartilage development: magnetic resonance imaging and polarized light microscopy. Eur Cell Mater 26:33–47; discussion 47–38.
9. Ytrehus B, Carlson CS, Ekman S. 2007. Etiology and pathogenesis of osteochondrosis. Vet Pathol 44:429–448.
10. van Weeren PR, Jeffcott LB. 2013. Problems and pointers in osteochondrosis: twenty years on. Vet J 197:96–102.
11. Bertone AL, Bramlage LR, McIlwraith CW, et al. 2005. Comparison of proteoglycan and collagen in articular cartilage of horses with naturally developing osteochondrosis and healing osteochondral fragments of experimentally induced fractures. Am J Vet Res 66:1881–1890.
12. Rejnö S, Strömberg B. 1978. Osteochondrosis in the horse. II. Pathology. Acta Radiol Suppl 358:153–178.
13. Khanna PC, Thapa MM. 2009. The growing skeleton: mr imaging appearances of developing cartilage. Magn Reson Imaging Clin N Am 17:411–421.
14. Dwek JR, Shapiro F, Laor T, et al. 1997. Normal gadolinium-enhanced mr images of the developing appendicular skeleton: part 2. Epiphyseal and metaphyseal marrow. AJR Am J Roentgenol 169:191–196.
15. Oeppen RS, Jaramillo D. 2003. Sports injuries in the young athlete. Top Magn Reson Imaging 14:199–208.
16. Connolly SA, Jaramillo D, Hong JK, et al. 2004. Skeletal development in fetal pig specimens: mr imaging of femur with histologic comparison. Radiology 233:505–514.
17. Menezes NM, Olear EA, Li X, et al. 2006. Gadolinium-enhanced mr images of the growing piglet skeleton: ionic versus nonionic contrast agent. Radiology 239:406–414.
18. Menezes NM, Connolly SA, Shapiro F, et al. 2007. Early ischemia in growing piglet skeleton: mr diffusion and perfusion imaging. Radiology 242:129–136.
19. Jaramillo D, Connolly SA, Mulkern RV, et al. 1998. Developing epiphysis: mr imaging characteristics and histologic correlation in the newborn lamb. Radiology 207:637–645.
20. Rivas R, Shapiro F. 2002. Structural stages in the development of the long bones and epiphyses: a study in the New Zealand white rabbit. J Bone Joint Surg Am 84A:85–100.
21. Fontaine P, Blond L, Alexander K, et al. 2013. Computed tomography and magnetic resonance imaging in the study of joint development in the equine pelvic limb. Vet J 197:103–111.
22. Li X, Majumdar S. 2013. Quantitative mri of articular cartilage and its clinical applications. J Magn Reson Imaging 38:991–1008.
23. Toth F, Nissi MJ, Wang L, et al. 2015. Surgical induction, histological evaluation, and mri identification of cartilage necrosis in the distal femur in goats to model early lesions of osteochondrosis. Osteoarthritis Cartilage 23:300–307.
24. Nissi MJ, Rieppo J, Toyras J, et al. 2006. T(2) relaxation time mapping reveals age- and species-related diversity of collagen network architecture in articular cartilage. Osteoarthritis Cartilage 14:1265–1271.
25. Dardzinski BJ, Laor T, Schmithorst VJ, et al. 2002. Mapping t2 relaxation time in the pediatric knee: feasibility with a clinical 1.5-t mr imaging system. Radiology 225:233–239.
26. Bourzac C, Alexander K, Rossier Y, et al. 2009. Comparison of radiography and ultrasonography for the diagnosis of osteochondritis dissecans in the equine femoropatellar joint. Equine Vet J 41:685–692.

1554527x, 2016, 10, Downloaded from https://onlinelibrary.wiley.com/doi/10.1002/jor.23176 by Portail BibCNRS INP, Wiley Online Library on [11/04/2025]. See the Terms and Conditions (https://onlinelibrary.wiley.com/terms-and-conditions) on Wiley Online Library for rules of use; OA articles are governed by the applicable Creative Commons License

27. Brown CP, Houle MA, Popov K, et al. 2013. Imaging and modeling collagen architecture from the nano to micro scale. Biomed Opt Express 5:233–243.
28. Hontoir F, Clegg P, Nisolle JF, et al. 2015. Magnetic resonance compositional imaging of articular cartilage: what can we expect in veterinary medicine? Vet J 205:11–20.
29. Dik KJ, Enzerink E, van Weeren PR. 1999. Radiographic development of osteochondral abnormalities, in the hock and stifle of dutch warmblood foals, from age 1 to 11 months. Equine Vet J Suppl 31:9–15.
30. van Weeren PR, Sloet van OO, Barneveld A. 1999. The influence of birth weight, rate of weight gain, and final achieved height and sex on the development of osteochondrotic lesions in a population of genetically predisposed warmblood foals. Equine Vet J Suppl 31:26–30.
31. UpRichard K, Elce YA, Piat P, et al. 2013. Outcome after arthroscopic treatment of lateral femoral trochlear ridge osteochondrosis in sport horses. A retrospective study of 37 horses. Vet Comp Orthop Traumatol 26:105–109.
32. Olstad K, Ytrehus B, Ekman S, et al. 2008. Epiphyseal cartilage canal blood supply to the tarsus of foals and relationship to osteochondrosis. Equine Vet J 40:30–39.
33. Barneveld A, van Weeren PR. 1999. Conclusions regarding the influence of exercise on the development of the equine musculoskeletal system with special reference to osteochondrosis. Equine Vet J Suppl 31:112–119.
34. Ekman S, Heinegard D. 1992. Immunohistochemical localization of matrix proteins in the femoral joint cartilage of growing commercial pigs. Vet Pathol 29:514–520.
35. Olstad K, Ytrehus B, Ekman S, et al. 2007. Early lesions of osteochondrosis in the distal tibia of foals. J Orthop Res 25:1094–1105.
36. Tchetina EV, Mwale F, Poole AR. 2014. Changes in gene expression associated with matrix turnover, chondrocyte proliferation and hypertrophy in the bovine growth plate. Acta Naturae 6:89–97.
37. Orth MW, Peters TL, Chlebek-Brown KA. 2000. Cartilage turnover in embryonic chick tibial explant cultures. Poult Sci 79:990–993.
38. Malemud CJ. 2006. Matrix metalloproteinases: role in skeletal development and growth plate disorders. Front Biosci 11:1702–1715.
39. Haeusler G, Walter I, Helmreich M, et al. 2005. Localization of matrix metalloproteinases, (mmps) their tissue inhibitors, and vascular endothelial growth factor (vegf) in growth plates of children and adolescents indicates a role for mmps in human postnatal growth and skeletal maturation. Calcif Tissue Int 76:326–335.
40. Mundlos S, Meyer R, Yamada Y, et al. 1991. Distribution of cartilage proteoglycan (aggrecan) core protein and link protein gene expression during human skeletal development. Matrix 11:339–346.
41. Lee ER, Lamplugh L, Davoli MA, et al. 2001. Enzymes active in the areas undergoing cartilage resorption during the development of the secondary ossification center in the tibiae of rats ages 0–21 days: i. Two groups of proteinases cleave the core protein of aggrecan. Dev Dyn 222:52–70.
42. Villemure I, Stokes IA. 2009. Growth plate mechanics and mechanobiology. A survey of present understanding. J Biomech 42:1793–1803.
43. Flachsmann R, Broom ND, Hardy AE, et al. 2000. Why is the adolescent joint particularly susceptible to osteochondral shear fracture? Clin Orthop Relat Res 381:212–221.
44. Klein TJ, Chaudhry M, Bae WC, et al. 2007. Depth-dependent biomechanical and biochemical properties of fetal, newborn, and tissue-engineered articular cartilage. J Biomech 40:182–190.
45. Martel M, Kiss S, Gilbert G, et al. 2016. Differences in the vascular tree of the femoral trochlear growth cartilage at osteochondrosis-susceptible sites in foals revealed by SWI 3T MRI. J Orthop Res 2016 Jan 6. doi: 10.1002/jor.23149. [Epub ahead of print].
46. Wosu R, Sergerie K, Levesque M, et al. 2012. Mechanical properties of the porcine growth plate vary with developmental stage. Biomech Model Mechanobiol 11:303–312.
47. Sankar WN, Matheney TH, Zaltz I. 2013. Femoroacetabular impingement: current concepts and controversies. Orthop Clin North Am 44:575–589.

SUPPORTING INFORMATION

Additional supporting information may be found in the online version of this article at the publisher's website.

1554527x, 2016, 10, Downloaded from https://onlinelibrary.wiley.com/doi/10.1002/jor.23176 by Portail BibCNRS INP, Wiley Online Library on [11/04/2025]. See the Terms and Conditions (https://onlinelibrary.wiley.com/terms-and-conditions) on Wiley Online Library for rules of use; OA articles are governed by the applicable Creative Commons License